Bending Rigidity of 2D Silica

C. Büchner,[1,*] S. D. Eder,[2,*] T. Nesse,[3,*] D. Kuhness,[1] P. Schlexer,[4] G. Pacchioni,[4,†]
J. R. Manson,[5,6] M. Heyde,[1] B. Holst,[2,‡,§] and H.-J. Freund[1,§]

[1]*Fritz-Haber-Institut der Max-Planck-Gesellschaft, Faradayweg 4-6, 14195 Berlin, Germany*
[2]*Department of Physics and Technology, University of Bergen, Allégaten 55, 5007 Bergen, Norway*
[3]*Department of Physics, NTNU Norwegian University of Science and Technology, NO-7491 Trondheim, Norway*
[4]*Department of Materials Science, Universitá di Milano-Bicocca, Via R. Cozzi, 55, Milan, Italy*
[5]*Department of Physics and Astronomy, Clemson University, Clemson, South Carolina 29634, USA*
[6]*Donostia International Physics Center (DIPC), Paseo Manuel de Lardizabal, 4, 20018 Donostia-San Sebastian, Spain*

(Received 19 October 2017; published 30 May 2018)

A chemically stable bilayers of SiO_2 (2D silica) is a new, wide band gap 2D material. Up till now graphene has been the only 2D material where the bending rigidity has been measured. Here we present inelastic helium atom scattering data from 2D silica on Ru(0001) and extract the first bending rigidity, κ, measurements for a nonmonoatomic 2D material of definable thickness. We find a value of $\kappa = 8.8$ eV $\pm$ 0.5 eV which is of the same order of magnitude as theoretical values in the literature for freestanding crystalline 2D silica.

DOI: 10.1103/PhysRevLett.120.226101

Two-dimensional materials form a class of materials with unique properties [1–5]. Several freestanding 2D materials are transferable and stable under various conditions [6,7]. The flexibility of 2D layers is a big advantage for a range of applications, for example flexible electronics [8], where both conductive and insulating layers are needed. Furthermore, it may be possible to tune properties such as the band gap, thermal conductivity, and resistivity through strain engineering [9].

One important mechanical property is the bending rigidity, κ, also known as flexural bending rigidity, flexural rigidity, bending modulus, or bending stiffness. The unit is Pascal $\times$ m^3 = Joule, with values for 2D materials customarily expressed in eV. For a plate the classical formula is [10]

$$\kappa = \frac{Yh^3}{12(1-\nu^2)}, \tag{1}$$

where Y is Young's modulus, h is the plate thickness, and ν is Poisson's ratio.

Several experiments exist on the measurement of elastic moduli for 2D materials, see for example Refs. [11,12], but to the best of the authors' knowledge single and few-layer graphene are the only 2D materials, up till now, where the bending rigidity has been measured directly. The experiments presented here are the first direct measurements of the bending rigidity on a nonmonoatomic 2D material. Following Eq. (1) it should be possible to obtain information about the elastic moduli from bending rigidity measurements and vice versa. However, this implies knowing h. For graphene, the value of h has proven to be ambiguous with different plausible values giving very different values for Young's modulus for carbon nanotubes. See, for example, Refs. [13–15]. This is known as the "Yakobson Paradox."

The first measurements of the bending rigidity of graphene were done in 2012 by investigating the snap-through behavior of freestanding graphene under electrostatic pressure. A value of $\kappa \approx 7.1$ eV was obtained [16]. More recently, the bending rigidity was determined by measuring the spring constant of a graphene cantilever yielding a value of 10^3 to 10^4 eV [17]. This very large value was attributed to ripples in the graphene.

In 2015 Al Taleb *et al.* introduced a new technique for measuring the bending rigidity of 2D materials: inelastic helium atom scattering (HAS) [18]. For a recent review on HAS see Ref. [19]. Using a recent theoretical approach [20] Al Taleb *et al.* extracted the bending rigidity of copper-supported single layer graphene from the ZA mode (flexural bending mode) in the phonon spectrum. They obtained $\kappa = 1.30$ eV $\pm$ 0.15 eV, the first experimental value in agreement with theoretical calculations [21,22]. They also determined the graphene-Cu coupling strength, $g = (5.7 \pm 0.4) \times 10^{19}$ N/m^3. Two advantages of using HAS are that the 2D material does not have to be freestanding, and the measurements are done over a large sample area. It is a prerequisite though, that the 2D material is weakly bound to the substrate [20]. For strongly bound systems, the phonon dispersion curves will share similarities with those of the uncoated substrate, particularly the

lowest energy mode will be similar to the substrate Rayleigh mode [23].

Here we use inelastic HAS to characterize the low-energy phonon modes of an Ru(0001)-supported mixed crystalline and vitreous 2D silica sample. From these measurements we extract the bending rigidity.

Silica is one of the most abundant materials on earth and the basis of a large class of glasses. It is relevant in modern technologies like semiconductor devices, optical fibers, and supports in industrial catalysis. Recently, 2D silica has garnered interest as a model glass for supporting catalytic systems, and as a promising 2D insulator layer. Crystalline [24] and vitreous 2D silica films [25,26] have been presented. For a recent review see Ref. [27].

HAS has previously been used to measure the surface boson peak on bulk, vitreous SiO_2 [28–31], as well as the surface structure, phonon spectrum, and surface Debye temperature of crystalline SiO_2 (quartz) [32–35].

The 2D silica sample was prepared at the Fritz Haber Institute Berlin: An Ru(0001) single crystal was cleaned by sputtering and annealing cycles until low-energy electron diffraction (LEED), Auger electron spectroscopy (AES), and scanning tunneling microscopy (STM) indicated a clean surface. By heating the sample to 1200 K in 2×10^{-6} mbar O_2 and letting it cool to room temperature in the same environment, a $3O(2 \times 2)$ cover was achieved. 1.95 ML Si was evaporated from a pure Si rod via an electron beam evaporator in 2×10^{-7} mbar O_2. The sample was annealed in 2×10^{-6} mbar O_2 in two steps: 1220 K for 10 min, and subsequently 1160 K for 5 min.

The resulting 2D silica sample was characterized in ultrahigh vacuum, using AES, LEED, and STM. Images can be seen in Fig. 1. The sample was subsequently removed from the UHV chamber and transported to the HAS setup. During transport, the sample was exposed to ambient conditions for more than 20 h.

The HAS experiments were carried out in MAGIE, the molecular beam apparatus at the University of Bergen. For a detailed description see Refs. [36,37]. The neutral helium beam was created by a free-jet expansion from a source reservoir through a 10 μm $\pm$ 0.5 μm diameter nozzle. The central part of the beam was selected by a skimmer, 410 μm $\pm$ 2 μm in diameter, placed 17.6 μm $\pm$ 0.5 μm in front of the nozzle. All experiments presented here were carried out on a room temperature sample $T_s = 296\,\mathrm{K} \pm 1\,\mathrm{K}$. The source-detector angle was held constant at $\theta_{SD} = 90°$. The rocking curves were measured with a room temperature beam ($T_n = 299$ K, $E_0 = 64$ meV), while for time-of-flight (TOF) measurements the beam was cooled to $T_n = 134$ K (measured beam energy $E_0 = 29$ meV). The stagnation pressure was $p_0 = 81$ bar for all TOF measurements. The beam spot size on the sample was 4 mm in diameter.

The sample was installed in the argon vented sample chamber which was then pumped down. The background pressure was around 1×10^{-9} mbar. A signal could be obtained from the sample without any initial cleaning. However, to ensure maximum intensity before measurements were done, the sample was heated to 675 K for 1 h in oxygen ($p_{O_2} = 2.2 \times 10^{-6}$ mbar). This improved the measured signal. A slight decline in reflected signal could be observed over a period of days. For this reason, the cleaning process was repeated before each day of measurements which restored the original reflectivity. The velocity spread of the beam was measured by TOF using a pseudorandom chopper [38].

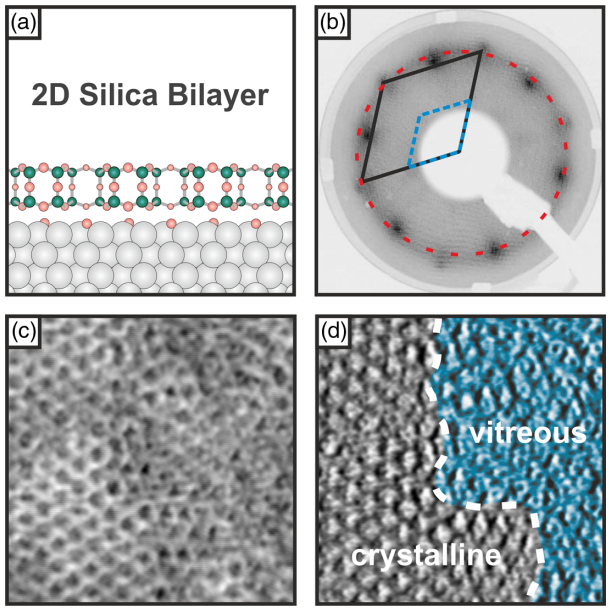

FIG. 1. Structural characterization of the metal-supported 2D silica sample: (a) Side view according to DFT model: Si atoms in green, O in red, Ru in gray. Note that the outermost layer consists of oxygen atoms. (b) Corresponding LEED image at an electron beam energy of 130 eV. The typical ring (red dotted line), corresponding to the vitreous 2D silica phase is visible together with a very faint (2×2) diffraction pattern (the reciprocal unit cell is indicated with a blue dashed line) which belongs to the small fraction of crystalline 2D silica. The black lines indicate the reciprocal unit cell of the Ru(0001) substrate, which has a lattice constant of 2.706 Å. (c) Topographic STM and (d) corresponding current image, showing a region with coexisting crystalline and vitreous 2D silica phase. Image sizes: 7 nm $\times$ 7 nm; tunneling parameters: bias voltage: 1.0 V, tunneling current: 130 pA.

Figure 1(c) shows an STM image of the 2D silica sample. Both vitreous and crystalline regions are visible, and the surface fraction of each phase was found to be close to 50% by inspection with STM. It should, however, be pointed out that it is only possible to inspect a very small fraction of the total area probed by HAS using STM. Figure 2 shows in-plane rocking scans performed at different azimuthal angles. The azimuthal angle $\phi = 0°$ corresponds to the ΓM direction of the Ru(0001) substrate. From Fig. 2 we see that the positions of the scattering peaks do not depend on the azimuthal direction and form a vitreous ring. This is the first time such a ring from a

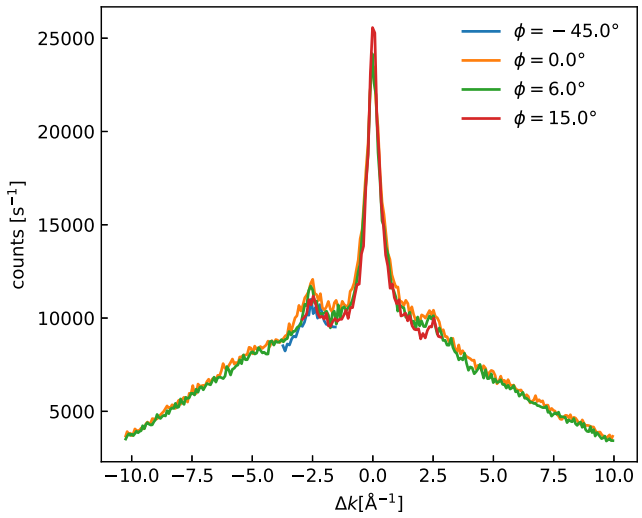

FIG. 2. Rocking scans measured on a mixed crystalline and vitreous silica film supported on an Ru(0001) substrate at different azimuthal angles for $T_0 = 300$ K. $\phi = 0°$ corresponds to the ΓM direction of the Ru(0001) substrate.

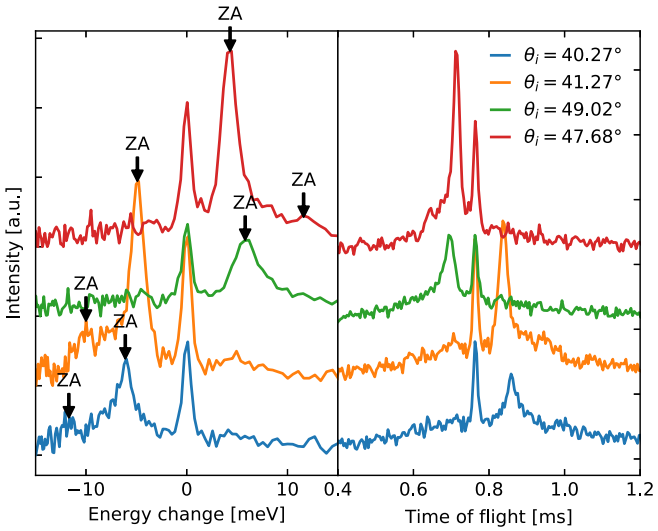

FIG. 3. The left panel shows a selection of energy converted time-of-flight spectra measured on a mixed crystalline and vitreous silica film supported on Ru(0001) taken in the direction ΓM with different incident angles θ_i. The right panel shows the corresponding raw time-of-flight spectra. The intensity is in arbitrary units, and a vertical shift has been introduced to discern between the different spectra. Annotations show ZA peaks.

vitreous substrate has been observed using HAS. Previous (unpublished) measurements by some of the authors of this Letter on bulk, vitreous SiO_2 only produced a very broad peak presumably due to the local surface roughness. The fact that the vitreous ring can be observed with HAS demonstrates the high quality of the atomically defined film over a macroscopic surface area. No crystalline diffraction pattern was observed, which suggests that the crystalline fraction of the film is smaller than suggested by STM measurements. This is also indicated by the LEED measurements [see Fig. 1(b)] where the (2×2) pattern corresponding to the crystalline fraction of the 2D silica is faint compared to the vitreous ring.

The radius of the vitreous ring in Fig. 2 leads to a characteristic length of 2.5 Å $\pm$ 0.1 Å. This is in excellent agreement with STM studies of other crystalline and vitreous 2D silica samples which show characteristic O-O distance of 2.7 Å $\pm$ 0.2 Å and 2.6 Å $\pm$ 0.2 Å, respectively [39]. It also agrees with the LEED image in Fig. 1(b). HAS probes the electron density distribution of the outermost surface layer. The measurements in Fig. 2 thus confirm the prediction of the model for 2D silica based on density functional theory (DFT), i.e., that the oxygen layer forms the outermost part of the film [see Fig. 1(a)].

Figure 3 shows typical TOF measurements and the corresponding energy converted TOF used to extract phonon energies. Based on the phonon energies, dispersion curves can be plotted, as shown in Fig. 4.

For a freestanding, isotropic membrane the flexural phonon mode is given by [41]

$$\omega_{\mathrm{ZA}}^{\mathrm{free}}(\Delta K) = \sqrt{\frac{\kappa}{\rho_{2\mathrm{D}}}}\Delta K^2 \tag{2}$$

where $\omega_{\mathrm{ZA}}^{\mathrm{free}}(\Delta K)$ is the frequency of the ZA-mode surface phonon for a given momentum ΔK, κ is the bending rigidity, and $\rho_{2\mathrm{D}}$ is the two-dimensional mass density of the membrane.

Based on DFT calculations, the 2D mass density of the free crystalline 2D silica is 1.63 mg m^{-2}, while it changes on the Ru(0001) substrate to 1.57 mg m^{-2}. Based on the analysis of STM measurements, the crystalline phase of the 2D silica indicates a 2D mass density of 1.68 mg m^{-2}, while for vitreous 2D silica it has been found to vary from 1.46 to 1.83 mg m^{-2}, with an average of 1.65 mg m^{-2} [42]. This is just twice the 2D mass density of graphene [43]. Evidently, the 2D mass density of the vitreous film fluctuates locally. In addition to this, 2D silica sometimes contains holes on the nm scale or larger. Special care was taken to make this sample "hole free," but we cannot exclude that there may have been some open areas. For the calculations we use the average mass density with an error bar: 1.65 mg m^{-2} $\pm$ 0.07 mg m^{-2}.

If the freestanding membrane is coupled to a substrate, this coupling will introduce a gap of frequency $\omega_0 = \sqrt{g/\rho_{2\mathrm{D}}}$, where g is the coupling strength between the membrane and the substrate:

$$\omega_{\mathrm{ZA}}^{\mathrm{coupled}}(\Delta K) = \sqrt{\frac{\kappa}{\rho_{2\mathrm{D}}}\Delta K^4 + \omega_0^2}. \tag{3}$$

Fitting the data in Fig. 4 with Eq. (3) we extract the bending rigidity for the 2D silica film. The results can be seen in Table I. The average value is $\kappa = 8.8$ eV $\pm$ 0.5 eV,

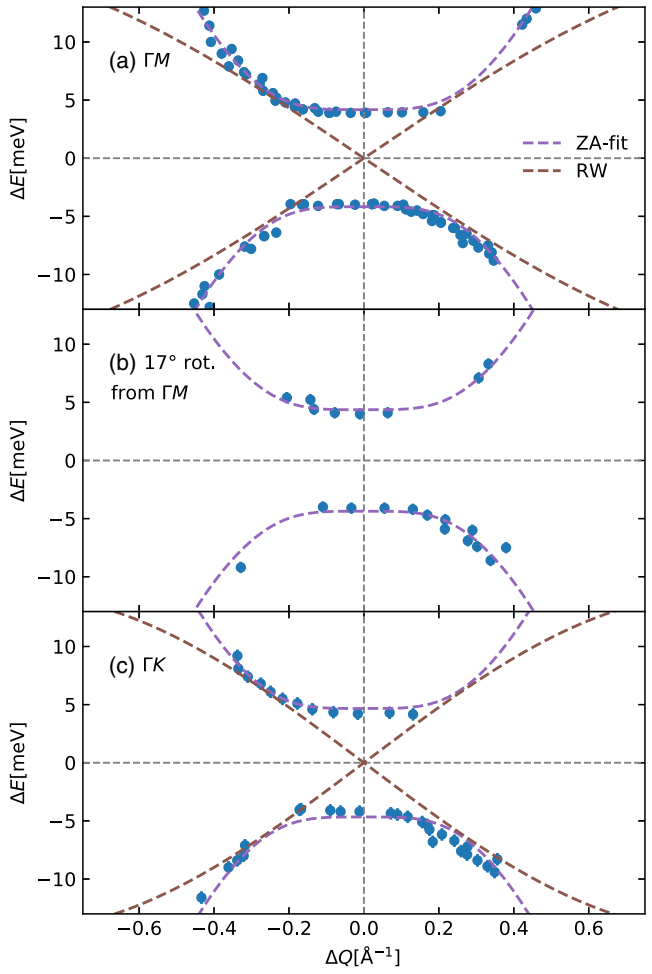

FIG. 4. Dispersion curves for mixed crystalline and vitreous 2D silica for the 2 azimuthal directions that fall along the major directions of the Ru(0001) substrate (a) ΓM and (c) ΓK, and one nonaligned direction (b) rotated 17° away from ΓM. The dashed purple line shows the fitted ZA mode using Eq. (3), while the dashed brown line shows the Rayleigh mode (RW) of the substrate [40]. As can be seen, the Rayleigh mode is not detected. The error bars show typical deviation of fit from the experimental data points.

which fits reasonably with two theoretical studies of freestanding, crystalline 2D silica: Gao *et al.* [9] and Schlexer and Pacchioni [44]. These theoretical studies were limited to a crystalline bilayer due to computational restrictions. The bending rigidity along the ΓK and ΓM directions, respectively, was found to be $\kappa = 12.5$ eV and 16.3 eV by Gao *et al.*, while Schlexer and Pacchioni obtained 17.3 eV and 22.9 eV. In the latter study it was found that because the shape of the calculated dispersion curve follows the form of Eq. (3) only in the limit $\Delta K \to 0$, the value of κ depends on the range of ΔK over which Eq. (3) is fitted. Increasing the ΔK range yielded least-squares fits with values of κ corresponding to those obtained in Ref. [9]. The discrepancy between the theoretical value for the bending rigidity and the value observed may be due to the fact that we are investigating a sample with both crystalline and vitreous areas. We do not measure any significant change in the bending rigidity when the sample is azimuthally rotated, showing that the isotropic behavior expected from the vitreous phase is dominating. We note that our experimental values agree well with the ΓK direction for theoretically calculated crystalline 2D silica, the lowest density direction. Furthermore, the sample may have defects in the form of holes. Recent experiments show a reduced bending rigidity of graphene deposited on sapphire compared to the theory [45]. The authors attribute this to defects. It has been reported that a defect density of 2% in graphene can cause a reduction in Young's modulus of a factor 2 [46] which in the classical picture of Eq. (1) would cause a factor 2 reduction in the bending rigidity.

TABLE I. Parameters describing the ZA mode found from a fit to the dispersion curves in Fig. 4 based on HAS measurements. The fit is performed using Eq. (3) and $\rho_{2D} = 1.65\ \mathrm{mg\,m^{-2}} \pm 0.07\ \mathrm{mg\,m^{-2}}$. The final column shows the parameters for a fit to the complete set of observed points.

Direction	ΓM	ΓM rot. 17%	ΓK	Full data set
κ [eV]	8.8 ± 0.5	8.4 ± 1.7	9 ± 1	8.8 ± 0.5
g [10^{19} N/m^3]	6.6 ± 0.5	7.2 ± 1.3	8 ± 1	7.2 ± 0.5

Table I also gives the values for the 2D silica—substrate coupling strength g found from the fit of Eq. (3) to the dispersion curves. Previously, the coupling constant of graphene on a weakly interacting Cu substrate was measured as $g = (5.7 \pm 0.4) \times 10^{19}$ N/m^3 [18]. The same authors have also reported a large change in the nominal bending rigidity for graphene on Ni substrates with a coupling constant of $g = (71.5 \pm 7) \times 10^{19}$ N/m^3 [47]. This shows that when the film gets more strongly bound, the model can no longer be used to predict the bending rigidity for a free film as also stated in the original paper [20]. The fact that we obtain a value for g that is quite similar to the value obtained for the weakly bound graphene/Cu system, confirms that we have weak coupling between the 2D silica film and the Ru(0001) substrate. This is also demonstrated by the fact that 2D silica films can be mechanically exfoliated and transferred from an Ru(0001) substrate to a different support as recently shown [7].

The set of TOF captured did not show any strongly visible peaks other than the ones assigned to the ZA mode. In particular, the Rayleigh mode of the Ru(0001) substrate was not detected (see Fig. 4), which is an additional confirmation that the 2D silica is very weakly bound to the substrate.

Finally, we return to Yakobson's Paradox. We use Eq. (1) to calculate the bending rigidity using a thickness value obtained by DFT and compare this with our experimentally determined value for bending rigidity. Further, we use our experimental value for bending rigidity to determine an

effective thickness and compare the two. Young's modulus for silica glass (fused silica) is 72 GPa and Poisson's ratio is 0.14 [48]. Based on STM measurements, values ranging from 3 Å to 5 Å have been reported for the apparent height of 2D silica on Ru(0001) substrates [7,49]. Height measurements in STM depend strongly on the local density of states, and the applied bias. Especially when heights are determined by scanning over a hole in the film, the tip interaction changes dramatically when going from the oxide to the metal surface, so that apparent height measurements may differ from the true height. For these reasons we performed DFT calculations, which gives an SiO_2 interlayer distance of 4.3 Å (distance between top and bottom oxygen nuclei). To get the film thickness, we add two times the nominal oxygen van der Waal radius of 1.5 Å [48], giving 7.3 Å. The real thickness is likely smaller, since element radii are typically shorter when they are involved in covalent bonds. Using this thickness in Eq. (1) we get a κ value of 15 eV. Using our measured bending rigidity we can calculate an effective thickness value using Eq. (1): this gives a value of 6.1 Å. As discussed above, defects in graphene have been shown to strongly reduce the value of Young's modulus [45,46]. Using our calculated thickness with our experimental bending rigidity in Eq. (1) we get a value for Y of 43 GPa, a reduction of around 40% compared to the bulk value. Further investigations on how defects affect the mechanical properties of 2D silica are needed, but our results suggest that there may in fact be a good agreement between DFT calculations of the film thickness and the thickness experimentally obtained using Eq. (1).

S. D. E., T. N., and B. H. acknowledge support from the Research Council of Norway, Projects No. 213453 and No. 234159. C. B. acknowledges funding from the German Research Council: Project No. 1109. Funding was also received from the European Research Council (ERC) under the European Union's Horizon 2020 research and innovation programme (Grant Agreement No. 669179). We thank Professor S. Sibener for assistance in implementing a pseudorandom chopper, and Bjørn Samelin and Werner Olsen for technical assistance.

[*]These authors contributed equally to this work.
[†]Corresponding author.
gianfranco.pacchioni@unimib.it
[‡]Corresponding author.
bodil.holst@uib.no
[§]These authors contributed equally to this work.

[1] K. S. Novoselov, D. Jiang, F. Schedin, T. J. Booth, V. V. Khotkevich, S. V. Morozov, and A. K. Geim, Proc. Natl. Acad. Sci. U.S.A. **102**, 10451 (2005).
[2] J. Hu, Z. Guo, P. E. Mcwilliams, J. E. Darges, D. L. Druffel, A. M. Moran, and S. C. Warren, Nano Lett. **16**, 74 (2016).
[3] G. Liu, W. Jin, and N. Xu, Angew. Chem., Int. Ed. Engl. **55**, 13384 (2016).
[4] N. G. Sahoo, Y. Pan, L. Li, and S. H. Chan, Adv. Mater. **24**, 4203 (2012).
[5] S. Yu, X. Wu, Y. Wang, X. Guo, and L. Tong, Adv. Mater. **29**, 1606128 (2017).
[6] S. Z. Butler, S. M. Hollen, L. Cao, Y. Cui, J. A. Gupta, H. R. Gutiérrez, T. F. Heinz, S. S. Hong, J. Huang, A. F. Ismach, E. Johnston-Halperin, M. Kuno, V. V. Plashnitsa, R. D. Robinson, R. S. Ruoff, S. Salahuddin, J. Shan, L. Shi, M. G. Spencer, M. Terrones, W. Windl, and J. E. Goldberger, ACS Nano **7**, 2898 (2013).
[7] C. Büchner, Z.-J. Wang, K. M. Burson, M.-G. Willinger, M. Heyde, R. Schlögl, and H.-J. Freund, ACS Nano **10**, 7982 (2016).
[8] S. J. Kim, K. Choi, B. Lee, Y. Kim, and B. H. Hong, Annu. Rev. Mater. Res. **45**, 63 (2015).
[9] E. Gao, B. Xie, and Z. Xu, J. Appl. Phys. **119**, 014301 (2016).
[10] E. Lifshitz, A. Kosevich, and L. Pitaevskii, *Theory of Elasticity*, 3rd ed. (Butterworth-Heinemann, Oxford, 1986).
[11] D. Akinwande, C. Brennan, J. Bunch, P. Egberts, J. Felts, H. Gao, R. Huang, J. Kim, T. Li, Y. Li, K. Liechti, N. Lu, H. Park, E. Reed, P. Wang, B. Yakobson, T. Zhang, Y. Zhang, Y. Zhou, and Y. Zhu, Extreme Mech. Lett. **13**, 42 (2017).
[12] K. Liu, Q. Yan, M. Chen, W. Fan, Y. Sun, J. Suh, D. Fu, S. Lee, J. Zhou, S. Tongay, J. Ji, J. B. Neaton, and J. Wu, Nano Lett. **14**, 5097 (2014).
[13] L. Wang, Q. Zheng, J. Z. Liu, and Q. Jiang, Phys. Rev. Lett. **95**, 105501 (2005).
[14] P. Pine, Y. E. Yaish, and J. Adler, Phys. Rev. B **89**, 115405 (2014).
[15] Y. Huang, J. Wu, and K. C. Hwang, Phys. Rev. B **74**, 245413 (2006).
[16] N. Lindahl, D. Midtvedt, J. Svensson, O. A. Nerushev, N. Lindvall, A. Isacsson, and E. E. B. Campbell, Nano Lett. **12**, 3526 (2012).
[17] M. K. Blees, A. W. Barnard, P. A. Rose, S. P. Roberts, K. L. McGill, P. Y. Huang, A. R. Ruyack, J. W. Kevek, B. Kobrin, D. A. Muller, and P. L. McEuen, Nature (London) **524**, 204 (2015).
[18] A. Al Taleb, H. K. Yu, G. Anemone, D. Farías, and A. M. Wodtke, Carbon **95**, 731 (2015).
[19] B. Holst and G. Bracco, in *Surface Science Techniques*, edited by G. Bracco and B. Holst (Springer, Berlin, Heidelberg, 2013), pp. 333–365.
[20] B. Amorim and F. Guinea, Phys. Rev. B **88**, 115418 (2013).
[21] K. N. Kudin, G. E. Scuseria, and B. I. Yakobson, Phys. Rev. B **64**, 235406 (2001).
[22] Y. Wei, B. Wang, J. Wu, R. Yang, and M. L. Dunn, Nano Lett. **13**, 26 (2013).
[23] D. Maccariello, D. Campi, A. Al Taleb, G. Benedek, D. Farías, M. Bernasconi, and R. Miranda, Carbon **93**, 1 (2015).
[24] D. Löffler, J. J. Uhlrich, M. Baron, B. Yang, X. Yu, L. Lichtenstein, L. Heinke, C. Büchner, M. Heyde, S. Shaikhutdinov, H.-J. Freund, R. Włodarczyk, M. Sierka, and J. Sauer, Phys. Rev. Lett. **105**, 146104 (2010).

[25] L. Lichtenstein, C. Büchner, B. Yang, S. Shaikhutdinov, M. Heyde, M. Sierka, R. Włodarczyk, J. Sauer, and H.-J. Freund, Angew. Chem., Int. Ed. Engl. **51**, 404 (2012).
[26] P. Y. Huang, S. Kurasch, A. Srivastava, V. Skakalova, J. Kotakoski, A. V. Krasheninnikov, R. Hovden, Q. Mao, J. C. Meyer, J. Smet, D. A. Muller, and U. Kaiser, Nano Lett. **12**, 1081 (2012).
[27] C. Büchner and M. Heyde, Prog. Surf. Sci. **92**, 341 (2017).
[28] W. Steurer, A. Apfolter, M. Koch, W. E. Ernst, B. Holst, E. Søndergård, and J. R. Manson, Phys. Rev. Lett. **99**, 035503 (2007).
[29] W. Steurer, A. Apfolter, M. Koch, W. E. Ernst, E. Søndergård, J. R. Manson, and B. Holst, Phys. Rev. Lett. **100**, 135504 (2008).
[30] W. Steurer, A. Apfolter, M. Koch, W. E. Ernst, E. Søndergård, J. R. Manson, and B. Holst, J. Phys. Condens. Matter **20**, 224003 (2008).
[31] W. Steurer, A. Apfolter, M. Koch, W. E. Ernst, E. Søndergård, J. R. Manson, and B. Holst, Phys. Rev. B **78**, 045427 (2008).
[32] W. Steurer, A. Apfolter, M. Koch, W. Ernst, and B. Holst, Surf. Sci. **602**, 1080 (2008).
[33] S. D. Eder, K. Fladischer, S. R. Yeandel, A. Lelarge, S. C. Parker, E. Søndergård, and B. Holst, Sci. Rep. **5**, 14545 (2015).
[34] W. Steurer, A. Apfolter, M. Koch, T. Sarlat, E. Søndergård, W. Ernst, and B. Holst, Surf. Sci. **601**, 4407 (2007).
[35] W. Steurer, A. Apfolter, M. Koch, W. E. Ernst, B. Holst, E. Søndergård, and S. C. Parker, Phys. Rev. B **78**, 035402 (2008).
[36] A. Apfolter, Master's thesis, Graz University of Technology, Institute of Experimental Physics, Austria, 2005.
[37] S. D. Eder, B. Samelin, G. Bracco, K. Ansperger, and B. Holst, Rev. Sci. Instrum. **84**, 093303 (2013).
[38] D. D. Koleske and S. J. Sibener, Rev. Sci. Instrum. **63**, 3852 (1992).
[39] L. Lichtenstein, M. Heyde, and H.-J. Freund, J. Phys. Chem. C **116**, 20426 (2012).
[40] J. Braun, K. Kostov, G. Witte, L. Surnev, J. Skofronick, S. Safron, and C. Wöll, Surf. Sci. **372**, 132 (1997).
[41] L. Karssemeijer and A. Fasolino, Surf. Sci. **605**, 1611 (2011).
[42] M. Heyde, G. H. Simon, and L. Lichtenstein, Phys. Status Solidi B **250**, 895 (2013).
[43] A. A. Green and M. C. Hersam, Nano Lett. **9**, 4031 (2009).
[44] P. Schlexer and G. Pacchioni (unpublished).
[45] G. Anemone, E. Climent-Pascual, H. K. Yu, A. Al Taleb, F. Jimenez-Villacorta, C. Prieto, A. M. Wodtke, A. De Andres, and D. Farias, RSC Adv. **6**, 21235 (2016).
[46] G. López-Polín, C. Gómez-Navarro, V. Parente, F. Guinea, M. Katsnelson, F. Pérez-Murano, and J. Gómez-Herrero, Nat. Phys. **11**, 26 (2015).
[47] A. Al Taleb, G. Anemone, D. Farías, and R. Miranda, Carbon **99**, 416 (2016).
[48] T. Bruno and P. Svoronos, *CRC Handbook of Basic Tables for Chemical Analysis* 3rd ed. (CRC Press, Boca Raton, FL, 2011).
[49] B. Yang, W. E. Kaden, X. Yu, J. A. Boscoboinik, Y. Martynova, L. Lichtenstein, M. Heyde, M. Sterrer, R. Wlodarczyk, M. Sierka, J. Sauer, S. Shaikhutdinov, and H.-J. Freund, Phys. Chem. Chem. Phys. **14**, 11344 (2012).